Correlated vortex pinning in slightly orthorhombic twinned $Ba(Fe_{1-x}Co_x)_2As_2$ single crystals: Possible shift of the vortex-glass/liquid transition

M. Marziali Bermúdez,[1] G. Pasquini,[1] S. L. Bud'ko,[2] and P. C. Canfield[2]

[1]*Departamento de Física, Universidad de Buenos Aires, and IFIBA, CONICET, Argentina*

[2]*Ames Laboratory, US DOE, and Department of Physics and Astronomy, Iowa State University, Ames, Iowa 50011, USA*

(Received 9 January 2013; revised manuscript received 21 February 2013; published 28 February 2013)

The interest in twin-boundary (TB) planes as a source of vortex pinning has been recently renewed with the discovery of the new iron-arsenide pnictide superconductors. In the family of compounds $Ba(Fe_{1-x}Co_x)_2As_2$ a structural transition from a tetragonal to orthorhombic lattice takes place for compounds with $x < x_{cr} \sim 0.065$. Approaching the critical doping, domain structure shrinks with sizes ultimately becoming comparable to vortex cores. In this work we investigate the changes in anisotropy produced by subtle differences in the Co doping level, in the neighborhood of the structural transition, in good-quality single crystals. Using a scaling approach we are able to determine the angular regions where correlated or uncorrelated disorder prevails. In the tetragonal samples ($x > x_{cr}$) there is no twinning and we find good agreement with the expected scaling function under uncorrelated disorder, with small anisotropy values similar to those reported in the literature. We show that in the orthorhombic samples ($x < x_{cr}$), TBs act as correlated disorder in a broad angular range. We propose that the observed angular dependence could be due to an increase in the vortex liquid-glass transition temperature.

DOI: 10.1103/PhysRevB.87.054515 PACS number(s): 74.70.Xa, 74.25.Uv, 74.62.Bf, 74.62.En

I. INTRODUCTION

Magnetic and transport properties in type-II superconductors are mainly determined by the underlying vortex physics. The vortex-vortex interaction in competition with quenched disorder and thermal fluctuations, together with material anisotropy, gives rise to a broad variety of vortex phases. If pinning is strong enough, a second-order vortex liquid-glass transition at a temperature $T_g(H)$ is expected, as it has been experimentally observed in high-T_c cuprates (HTSs).[1,2] The variety of phases and dynamic regimes are mainly determined by the strength and topology of the quenched disorder. In this context, correlated disorder due to extended linear or planar defects is particularly relevant since they constitute the most efficient way to pin vortices. The competition between pinning and elastic forces is known to give rise to history effects that disappear when correlated disorder prevails.[3] Moreover, correlated defects with broken symmetry (as lines or planes) can modify the glass phase onto a Bose-glass phase, with a preferential magnetic field direction for which the transition temperature $T_g(H)$ increases.[1,4]

Correlated linear defects can be artificially created, for example, by heavy-ion irradiation that produces columnar defects.[5] On the other hand, planar defects are formed naturally in anisotropic superconductors, where the atomic layers are themselves a source of planar correlated disorder. However, for practical geometrical reasons the magnetic field is generally applied perpendicular to the layers. Twin boundaries, present in materials that undergo tetragonal to orthorhombic phase transitions, become planar defects for this geometry. The efficiency of twin boundaries as pinning centers has been extensively probed in YBCO crystals,[6] and the correlated nature of this pinning has been evidenced by measuring the angular dependence of the transport properties: A sharp peak in the resistivity together with a change in the universality class of the glass to liquid transition when the magnetic field is applied at small angles away from the direction of the correlated defects has been observed.[7] By magnetization[8,9] and ac susceptibility measurements,[10] it has been shown that correlated defects modify the expected intrinsic angular dependence (due to the material anisotropy) over a larger angular region. This fact has been explained in terms of formation of vortex staircases[9,12] with vortex segments aligned with the defects but the mean vortex direction following that of the applied magnetic field.

The interest in TBs has been recently renewed with the discovery of the new iron-arsenide pnictides superconductors.[13] In the family of compounds $Ba(Fe_{1-x}Co_x)_2As_2$ a structural transition from a tetragonal to orthorhombic lattice correlated with a magnetic transition occurs at a temperature T_s that decreases with increasing x, crossing the superconducting transition temperature T_c at $x \sim 0.065$.[14,16,17] Approaching this critical doping, domain structure becomes more intertwined and fine, due to a decrease in the orthorhombic distortion δ. A peak of maxima critical current density is observed in the range where the structural domain size becomes finely spaced.[17] Although due to a suppression of δ, structural domains cannot be optically resolved for $x > 0.054$, approaching the critical doping, sizes ultimately would become comparable to the size of vortex cores.[17] Direct observations in samples with $x \sim 0.05$[18] suggest that, as in YBCO crystals,[19] TBs could also serve as channels that facilitate the vortex mobility in one direction but inhibit motion in the crossing direction. However, no evidence of the correlated nature of pinning produced by TBs in these new compounds has been provided up to now. Moreover, these compounds offer the unique possibility to study the anisotropy modification in the crossover from tetragonal-untwinned to orthorhombic-twinned samples by a subtle change in the Co doping.

In this work we investigate the superconducting anisotropy in high-quality single crystals with different Co doping levels close to x_{cr}, in the neighborhood of the superconducting transition. Using a scaling approach we are able to determine the angular regions where correlated or uncorrelated disorder prevails. From the particular characteristics of the ac response in these samples and its correlation with magnetization

measurements we conclude that, at least in the region of low fields (up to 1 T), TBs shift the vortex liquid-glass transition to higher temperatures in a broad angular range.

II. EXPERIMENTAL

Single crystals of $Ba(Fe_{1-x}Co_x)_2As_2$ were grown from FeAs flux from a starting load of metallic Ba, FeAs, and CoAs, as described in detail elsewhere.[14] Samples are thin platelets with the larger area perpendicular to the c axis, with typical areas around 2–5 mm^2 and thickness $d \sim 0.1$ mm. In this study samples from 3 batches with different Co doping have been measured: batches with $x = 0.074$ and $x = 0.067$ are near the lower doping level belonging to the tetragonal phase, and a batch with $x = 0.062$, near the upper doping level corresponding to the orthorhombic twinned phase.

Magnetization and ac characterization (up to $f = 1$ kHz) where done in a Quantum Design MPMS with ac accessory, whereas angular ac susceptibility measurements (1 kHz $< f <$ 100 kHz) where carried out in a Janis continuous flow He cryostat with a homemade adaptation to work as a susceptometer. Samples are mounted inside a small solenoid that provides a transverse ac field parallel to the c axis. The dc field is provided by an electromagnet that can be rotated with a precision of $\Delta\theta \simeq 0.2^\circ$. The absolute angle relative to the c axis is obtained from the symmetry of the response, and can be ensured within a $\Delta\theta \simeq \pm 1^\circ$. Notice that in this experimental setup the geometry determining the relationship between the intrinsic transport properties, the applied ac field and the ac susceptibility (sometimes associated with a demagnetization factor), is independent of the dc field direction for $H \gg H_{c1}$. A sketch of the experimental geometry with the definition of the θ angle is shown in the inset of Fig. 1.

The in-phase and out-of-phase first harmonic component of the ac susceptibility, χ' and χ'', have been normalized using the zero field response at low temperatures, in such a way that $\chi' = -1$ and $\chi'' = 0$ when there is complete ac screening, and both components are 0 in the normal state.

III. RESULTS AND DISCUSSION

Figure 1(a) shows typical normalized in-phase χ' and out of phase χ'' first harmonic ac susceptibility components at zero dc field, for samples with different doping levels as a function of temperature. Sharp ac transitions ($\Delta T \sim 0.5$ K with a 10%–90% criterium) reveal high-quality crystals. With increasing ac amplitude h_a, as expected, the maximum in χ'' increases and moves to lower temperatures and $\chi'(T)$ curves are slightly broadened. Figure 1(b) shows $\chi'(T)$ and $\chi''(T)$ for a a larger twinned crystal (measured in the MPMS, at a lower frequency) at various dc fields applied parallel to the c axis. As reported in other works,[21] in these compounds the application of a dc field mainly shifts the transition to a lower temperature, without significative broadening; only the low-temperature tails show significative difference. This fact is due to the very strong pinning, which inhibits vortex motion: Once the system enters the solid (or glass) phase, vortices are strongly pinned and typical ac fields (amplitudes h_a around a few Oe) are almost completely screened. The phenomenology displayed in Figs. 1(a) and 1(b) is very

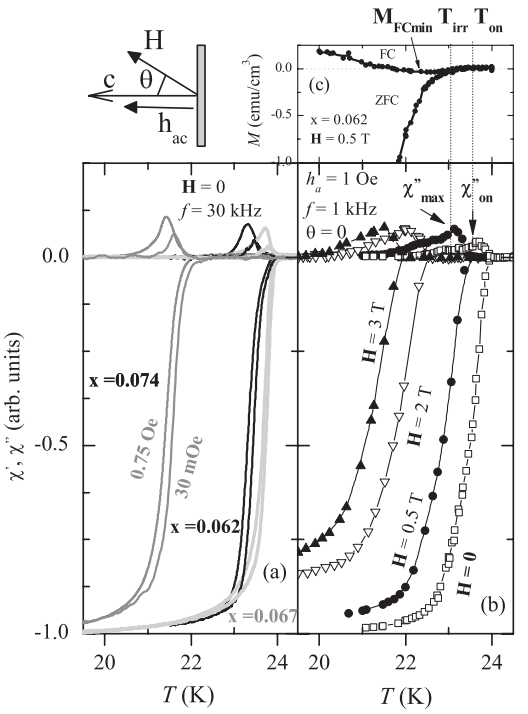

FIG. 1. Sharp ac transitions without significative enlargement with increasing dc and ac fields are observed. (a) Normalized in-phase χ' and out-of-phase χ'' at $H = 0$, for samples with various Co doping, as a function of T recorded with different ac amplitudes. (b) $\chi'(T)$ and $\chi''(T)$ for a larger crystal with $x = 0.062$ at various dc fields. (c) ZFC and FC $M(T)$ curves at $H = 5000$ Oe. Arrows in (b) and (c) identify examples of typical points plotted in the phase diagram of Fig. 5 in curves recorded at $H = 5000$ Oe (black dots). Inset: Sketch of the experimental geometry, where the gray rectangle represents a sample cross section.

different from that occurring in the weakly pinned vortex lattice of HTSs, or other traditional superconductors, where a significative enlargement of the ac susceptibility transition with increasing dc and ac fields is observed.

Taking into account the narrowness and subtle dependence of the observed transitions, we have chosen T swept curves in slow cooling ramps as the best way to perform our experiments in the homemade susceptometer. Dependencies with other variables at a given temperature have then been obtained by slicing the corresponding $\chi'(T)$ curves. Figure 2 shows examples of two groups of curves at various dc fields H [Fig. 2(a)] and various orientations of the dc field θ [Fig. 2(b)]; θ is the angle between the field direction and the c axis. The points where the vertical lines at a fixed temperature cross each curve are used to obtain $\chi'(H)$ and $\chi'(\theta)$ dependencies.

Figure 3 shows examples of the resulting curves obtained with the above procedure, in samples with different Co doping. Figure 3(a) shows $\chi'(H)$ curves, and Fig. 3(b) shows $\chi'(\theta)$ dependencies. The structural transition is expected to occur above T_c for the underdoped sample [$x = 0.062$, dark gray circles in Fig. 3(a)],[14] so it is expected to be slightly orthorhombic during the superconducting transition, with very narrow domains between TBs; the overdoped samples ($x = 0.067$, black symbols, and $x = 0.072$, light gray symbols), instead, have a tetragonal structure at all temperatures,

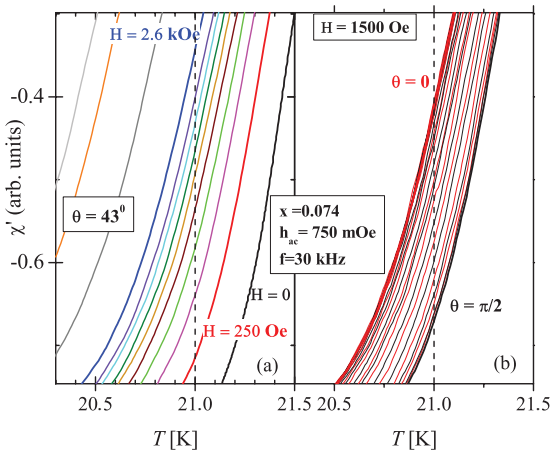

FIG. 2. (Color online) Example of $\chi'(T)$ curves recorded in slow cooling T ramps at (a) various dc fields H and (b) various orientations of the dc field θ, in an untwinned sample. A Savitzky-Golay filter has been applied in order to smooth the high-frequency uncorrelated random noise in the temperature and susceptibility voltage signals. The χ' values corresponding to the intersection between the vertical dashed lines ($T = 21$ K) with each $\chi'(T)$ curve have been used to build the curves shown in Fig. 3 (black squares).

without TBs. It can be readily seen that the formation of TBs causes a dramatic change in the angular dependence. The dip in the angular dependence occurs at all the measured temperatures. As can be seen in the inset of Fig. 3, the full $\chi(T)$ curves recorded around $\theta = 0$ (red line) shift to higher temperatures. In the following we analyze the measured angular dependence in the framework of the scaling approach[1] proposed in the 1990s to study anisotropic HTS materials.

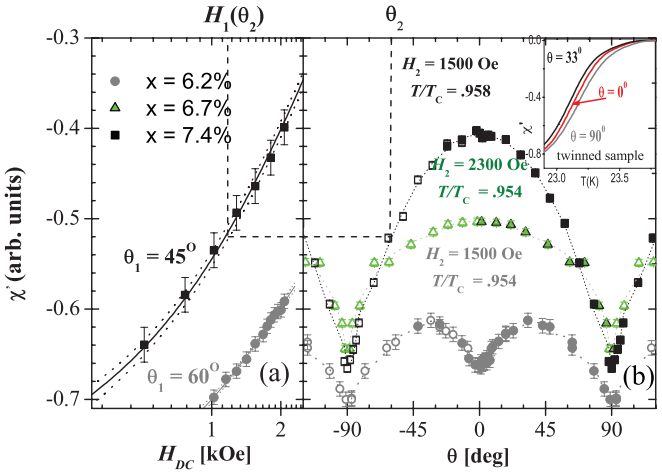

FIG. 3. (Color online) Examples of curves obtained by ex-tracting data for recorded $\chi'(T)$ curves (a) $\chi'(H)$ at fixed T and θ in two samples. (b) $\chi'(\theta)$ curves at fixed T and H in untwinned ($x = 0.067$ and $x = 0.074$) and twinned ($x = 0.062$) samples. A dramatic change caused by TBs is observed. Continuous and dotted lines in panel (a) show the interpolation functions $\chi'(H)$ and the corresponding confidence bands. Dashed line connecting both panels schematizes the definition of $H_1(\theta)$ in the scaling procedure (Fig. 4). Inset: $\chi'(T)$ curves in the twinned samples corresponding to 3 directions of the dc field $H = 1500$ Oe. Around $\theta = 0$ the full curves shift to higher temperatures.

In 3D superconductors the anisotropic parameter is defined as $\varepsilon = \xi_c/\xi_{ab}$, where $\xi_{c,ab}$ are the coherence lengths in the direction of the corresponding crystallographic axis. The angular dependence of any property (resistivity, critical current density, etc.), in principle, could be obtained by solving the GL equations with an effective mass along the c axis $M = m/\varepsilon$ in the presence of the quenched disorder distribution. In practice, this is generally not possible. However, when uncorrelated random disorder prevails, in the range of large $\kappa = \lambda/\xi$ and fields $H \gg H_{c1}$, a scaling approach allows the recovery of the GL solutions for isotropic materials by applying simple scaling rules. The scaling rule is particularly simple at a fixed temperature: Any intrinsic property Q will scale with the same property in the isotropic case $\breve{Q}$ as

$$Q(\theta, H) = s_Q \breve{Q}(\varepsilon_\theta H),$$

where $\varepsilon_\theta^2 = \varepsilon^2 \sin^2\theta + \cos^2\theta$ and $s_Q = 1, \varepsilon$, or $1/\varepsilon$ (depending on the quantity Q). In multiband superconductors, recent work[15] has shown that the scaling will still be valid by including a temperature-dependent effective mass, consistent with experimental results[22] reporting a T-dependent anisotropy in these compounds.

The approach will be valid if boundary conditions affecting Q are not modified when varying θ. This is the case of the ac susceptibility χ in our experimental situation, where the direction of the ac field relative to the sample geometry is unchanged when the dc field is rotated. Therefore, if uncorrelated random disorder prevails, the angular dependence of the ac susceptibility at fixed T will be related to the field dependence through the following scaling rule:

$$\chi(\theta_1, H_1) = \chi(\theta_2, H_2) \iff H_1 = \frac{\varepsilon_{\theta_2}}{\varepsilon_{\theta_1}} H_2.$$

As tilt and compression elastic modulus are very similar,[1] no other reasons beyond the material anisotropy are expected to affect $\chi(\theta)$.

We have then investigated whether the scaling holds in the different samples. With this scope, the $\chi'(\theta_1, H)$ and $\chi'(\theta, H_2)$ dependencies have been obtained by slicing curves measured at various dc fields H and fixed angle θ_1, and at fixed dc field H_2 and various angles θ, respectively. Results are shown in in Figs. 3(a) and 3(b), respectively. We have deliberately avoided the crystallographic directions to choose θ_1 for reasons that will become apparent below. The former was interpolated by means of a least-squares polynomial fit and, for each θ in the latter, we estimated the corresponding magnetic field $H_1(\theta)$ such that $\chi'(\theta_1, H_1(\theta)) = \chi'(\theta, H_2)$, i.e. the field necessary at a given angle to recover the same response at another angle and a given field. A sketch illustrating the meaning of $H_1(\theta)$ for a single point θ_2 corresponding to the sample with $x = 0.074$ is shown in Fig. 3(b) with dashed lines (notice that both panels have the same vertical scale, so the horizontal line connects points with identical χ' value). Examples of the resulting $H_1(\theta)/H_2$ for samples with different Co doping are shown in Fig. 4.

We have noticed that it is not possible to fit the data in the whole angular range with a scaling function of the form

$$\frac{H_1(\theta)}{H_2} = \frac{\varepsilon_\theta}{\varepsilon_{\theta_1}} = \frac{\sqrt{\varepsilon^2 \sin^2\theta + \cos^2\theta}}{\sqrt{\varepsilon^2 \sin^2\theta_1 + \cos^2\theta_1}}.$$

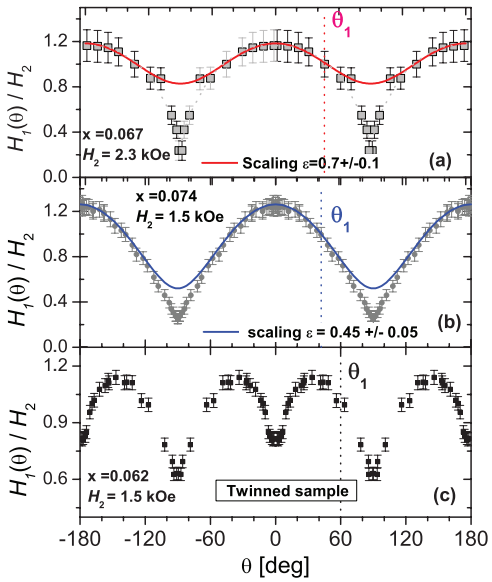

FIG. 4. (Color online) Examples of the resulting $H_1(\theta)/H_2$ for samples with different Co doping, $H_1(\theta)$ being defined as the "effective field" for which $\chi(\theta_1, H_1(\theta)) = \chi(\theta, H_2)$. The chosen angles θ_1 are indicated with vertical dashed lines. Continuous lines show the scaling function obtained for untwinned samples [panels (b) and (c)] in the region $\theta < \theta_c$ (see text). In the twinned sample [panel (a)] TBs act as sources of correlated disorder in a broad angular range.

However, in the tetragonal samples, a good fitting can be achieved by restricting the angular region. In order to obtain this region and the best ε, we have performed least-squares fits to the data; comparing the reduced χ^2 for fits resulting from different angular intervals, we observed a sharp rise at certain cutoff angle θ_c (around 60°–70° depending on the sample). After discarding the points beyond θ_c, a Monte Carlo method was applied to estimate the value and standard deviation of ε. A good agreement with the expected scaling function holds [continuous lines in Fig. 4, panels (a) and (b)] in the range $\theta < \theta_c$ with $\varepsilon = 0.7 \pm 0.1$ and $\varepsilon = 0.45 \pm 0.05$ for $x = 0.067$ and $x = 0.074$, respectively. These small anisotropy values are in good agreement with those reported in other works,[14,22,23] obtained by other methods.

The scaling fails when the field direction approaches the ab planes, similarly to that observed in HTS cuprates,[9,10] where this fact is ascribed to the modulation of the superconducting parameter with atomic layers. Intrinsic pinning has been observed also in Co-doped $BaFe_2As_2$ films at low T.[11] In the present case, the relatively large ξ_c (more than 40 Å in this temperature range[16]) compared with the distance between FeAs planes (∼7 Å) suggests that the modulation will be strongly smeared. However, the smooth modulation could be enough to break the random pinning hypothesis, necessary to validate the scaling rule. In any case, the loss of the scaling beyond θ_c in our experiments is an experimental fact.

On the other hand, in the twinned sample ($x = 0.062$), $H_1/H_2(\theta)$ drops for $\theta \lesssim 40°$, and no scaling is possible. The procedure has been repeated at other temperatures, as well as rotating the samples in the basal plane. Beside some marginal quantitative differences, the angular response shows the same qualitative features. From these results, it is clear that defects present in tetragonal compounds can be considered as random disorder far away from the direction of the ab planes and that TBs act as sources of correlated disorder.

The above analysis has been performed making use of general scaling concepts, without entering into the underlying physics. From now on, we discuss the possible origin of the ac susceptibility response and consequently the role that TBs may play at high temperatures in these samples. The relationship between the ac response in superconductors and the underlying vortex physics has been extensively discussed for many years. Excluding the phase transition regions, the contribution from changes in the equilibrium magnetization (due to the small changes in the magnetic field) is negligible compared with the contribution from moving vortices. Typical ac fields move vortices over short distances, but these small displacements propagate into the sample over a macroscopic distance known as the ac penetration depth λ_{ac}, forming time-dependent profiles. The nonlinear ac response $\lambda_{ac}(h_a, \omega, T, B)$ can be linked with the effective critical current density $J_c(\omega, T, B)$, and the possible frequency dependence is a consequence of thermal activated creep. For thin samples in transversal geometry in a Bean critical state (with or without creep), at fixed temperature and field, the nonlinear ac susceptibility scales with h_a/d for a given geometry (disk, stripe, etc.).[20] We have compared the nonlinear response taken at different ac amplitudes, in samples with different thickness (cleaved from the same crystal and having the same area and shape). In all the temperature range, we have not found a h_a/d scaling, indicating the absence of a critical state. Our results are consistent with those reported in Ref. 21, where the frequency dependence of the nonlinear ac susceptibility does not correspond with that expected from a thermal activated process. In this reference, authors claim that the ac susceptibility response in these compounds would be mainly associated with the dynamic response in the critical region of the vortex liquid-glass phase transition.

With the aim to investigate the consistence of our experimental results with the proposed scenario, we have located the ac susceptibility characteristic points in a phase diagram obtained by magnetization results. Both kinds of measurements have been carried out in the MPMS (QD), with the magnetic field H parallel to the twin planes ($\theta = 0$), in two large twinned crystals from the same batch (black and gray symbols in Fig. 5).

The magnetic moment $m = MV$ has been measured at fixed T as a function of H, and the characteristic points $H_{min}(T)$, $H_p(T)$, and $H_{irr}(T)$ have been identified (see example in the inset of Fig. 5) and plotted in the phase diagram (main panel) in full diamonds, circles, and up triangles, respectively. From previous results in similar samples,[24–26] $H_{min}(T)$ and $H_p(T)$ can be related to changes in the pinning regime and creep mechanism. $H_{irr}(T)$ depends on the resolution, indicating the field where the upper and lower branches of the magnetization loops $M(H)$ become indistinguishable.

On the other hand, from $M(T)$ curves at fixed applied H [example in Fig. 1(c)], we have identified the onset of the diamagnetic shielding $T_{on}(H)$ [related in the literature to $T(H = H_{c2})$][21,26] and the temperature $T_{irr}(H)$ where $M(T)$ curves recorded in ZFC and FC procedures become identical (solid squares and down triangles in Fig. 5). In curves recorded in cooling procedures (FC), we have also observed

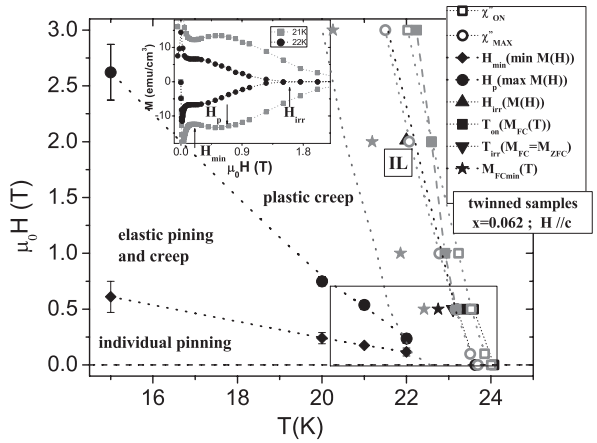

FIG. 5. Inset: Magnetization loops $M(H)$ at fixed T in a twinned sample. Main panel: Phase diagram built with magnetization (full symbols) and ac susceptibility (open symbols) results in two twinned samples (gray and black symbols). Examples of the definition of the plotted quantities are shown in the inset and in Fig. 1(b). The IL (up and down triangles) coincides approximately with $\chi''_{\max}$ (open circles) and lies near the onset of the diamagnetic signal (squares). The rectangle in the right bottom corner indicates the region where angular measurements have been performed.

a strange minimum in $M(T)$ (stars in Fig. 5) below which the magnetization increases and even becomes positive [see Fig. 1(c)], the origin of these striking features being beyond the scope of this paper.

The characteristic points obtained from ac susceptibility measurements are plotted with open symbols in the diagram: squares represent the onset of the dissipation and circles the maximum in χ' at $f = 1$ kHz and $h_a = 1$ Oe; the dotted line delimits the region where the normalized χ'' is above a threshold value ($\sim$0.01) and χ' abruptly increases (at these particular f and h_a).

The H-T phase diagram presented in Fig. 5 clearly shows that the so-called "irreversibility line" (IL) obtained by magnetic measurements at fixed T (up triangles) matches with that obtained at fixed H (down triangles) in both samples and coincides approximately with the maximum in χ''. Below this line, irreversibility is measurable and a vortex glass phase is expected to exist. This coincidence together with the lack of a typical critical state response is consistent with the possibility that in these samples the ac transition was related to the vortex glass-liquid phase transition. The most interesting feature is that, contrary to that observed in other pnictides, including the $Ba(Fe_{1-x}Co_x)_2As_2$ family,[16,21,24–26] the IL lies very near the onset of the diamagnetic signal measured through both magnetization (solid squares) and ac susceptibility (open squares) techniques. The vortex liquid phase (if there is one) seems to be very narrow, at least for fields below $H = 2$ T, a condition that includes all the region where angular measurements have been performed (rectangle in the right bottom corner). It seems that for higher fields this region tends to be enlarged, but unfortunately experimental problems prevented us from obtaining good susceptibility curves at higher fields.

Therefore, our results should indicate that the dip in $\chi'(\theta)$ displayed in Fig. 3 could be due to a shift of the $T_g(H)$ line to higher temperatures, with a stretching of the vortex liquid phase. Such a shift is expected to occur in the presence of correlated disorder in the Bose-glass phase,[1,4] below a small lock-in angle. However, the dip in Figs. 3 and 4 persists up to $\theta \sim 40^\circ$. In the proposed scenario, in all the angular range where vortices are expected to accommodate in TB planes (probably forming staircases), there would be a continuous shift of the $T_g(H)$ line.

IV. CONCLUSIONS

The superconducting anisotropy in good-quality $Ba(Fe_{1-x}Co_x)_2As_2$ single crystals with different Co doping levels close to x_{cr}, in the neighborhood of the superconducting transition, has been investigated. We observe that the formation of twin boundaries (TBs) in samples with $x = 0.062$, near the upper doping level corresponding to the orthorhombic twinned phase, causes a dramatic change in the angular dependence.

Using a scaling approach we are able to determine the angular regions where uncorrelated disorder prevails. From this point of view, defects present in tetragonal compounds can be considered as random disorder. In these samples, small anisotropy values ($\varepsilon \sim 0.5$–0.7) were obtained, in good agreement with those reported in the literature. The scaling fails approaching the ab planes, suggesting that the smeared modulation of the superconducting parameter is enough to break the pinning isotropy. On the other hand, in the orthorhombic samples, we observe that TBs act as sources of correlated disorder in a broad angular range.

The characteristics of the nonlinear ac response, together with the coincidence between the maximum in the ac dissipation and the irreversibility line, indicate that the ac susceptibility response could be mainly associated with the dynamic response in the critical region of the vortex liquid-glass phase transition. Our results could indicate that twin boundaries shift the temperature of the glass transition $T_g(H)$ to higher temperatures, with a stretching of the vortex liquid phase. A scaling with frequency in the linear regime (unable to be performed with our setup) could confirm this hypothesis. Interesting insights might be obtained by studying the angular dependence of the critical current density as a function of temperature in underdoped samples with slightly higher Co content, so that $T_s \lesssim T_c$, where both structural phases belonging in the superconducting state should become accessible in the same sample. Angular transport measurements as well as direct observations of vortex arrangement could also reveal valuable information.

ACKNOWLEDGMENTS

This work was partially supported by UBACyT (x166, 676), CONICET (PIP 112-200801-00930) and ANPCyT (PICT 753). Research performed at Ames Laboratory (P.C.C. and S.L.B.) was supported by the US Department of Energy, Office of Basic Energy Science, Division of Materials Sciences and Engineering. Ames Laboratory is operated for the US Department of Energy by Iowa State University under Contract No. DE-AC02-07CH11358. We would like to acknowledge N. Ni and A. Thaler for sample preparation and R. Prozorov and V. Bekeris for reviewing the draft and useful comments.

[1]G. Blatter, M. V. Feigel'man, V. B. Geshkenbein, A. I. Larkin, and V. M. Vinokur, Rev. Mod. Phys. **66**, 1125 (1994).
[2]P. L. Gammel, L. F. Schneemeyer, J. V. Waszczak, and D. J. Bishop, Phys. Rev. Lett. **61**, 1666 (1988).
[3]G. Pasquini, D. Luna, and G. Nieva, Phys. Rev. B **76**, 212302 (2007).
[4]D. R. Nelson and V. M. Vinokur, Phys. Rev. Lett. **68**, 2398 (1992).
[5]L. Civale, A. D. Marwick, T. K. Worthington, M. A. Kirk, J. R. Thompson, L. Krusin-Elbaum, Y. Sun, J. R. Clem, and F. Holtzberg, Phys. Rev. Lett. **67**, 648 (1991).
[6]The first evidence: L. Ya. Vinnikov, L. A. Gurevich, G. A. Emelchenko, and Yu. A. Ossipyan, Solid State Commun. **67**, 421 (1988).
[7]S. A. Grigera, E. Morré, E. Osquiguil, C. Balseiro, G. Nieva, and F. de la Cruz, Phys. Rev. Lett. **81**, 2348 (1998).
[8]A. A. Zhukov, G. K. Perkins, J. V. Thomas, A. D. Caplin, H. Kupfer, and T. Wolf, Phys. Rev. B **56**, 3481 (1997).
[9]A. Silhanek, L. Civale, S. Candia, G. Nieva, G. Pasquini, and H. Lanza, Phys. Rev. B **59**, 13620 (1999).
[10]G. Pasquini, L. Civale, H. Lanza, and G. Nieva, Phys. Rev. B **65**, 214517 (2002).
[11]B. Maiorov, T. Katase, I. O. Usov, M. Weigand, L. Civale, H. Hiramatsu, and H. Hosono, Phys. Rev. B **86**, 094513 (2012).
[12]J. A. Herbsommer, G. Nieva, and J. Luzuriaga, Phys. Rev. B **62**, 3534 (2000).
[13]Y. Kamihara, T. Watanabe, M. Hirano, and H. Hosono, J. Am. Chem. Soc. **130**, 3296 (2008); M. Rotter, M. Tegel, and D. Johrendt, Phys. Rev. Lett. **101**, 107006 (2008).
[14]N. Ni, M. E. Tillman, J.-Q. Yan, A. Kracher, S. T. Hannahs, S. L. Bud'ko, and P. C. Canfield, Phys. Rev. B **78**, 214515 (2008).
[15]M. Kidszun, S. Haindl, T. Thersleff, J. Hanisch, A. Kauffmann, K. Iida, J. Freudenberger, L. Schultz, and B. Holzapfel, Phys. Rev. Lett. **106**, 137001 (2011).
[16]P. C. Canfield and S. L. Bud'ko, Annu. Rev. Condens. Matter Phys. **1**, 27 (2010).
[17]R. Prozorov, M. A. Tanatar, N. Ni, A. Kreyssig, S. Nandi, S. L. Bud'ko, A. I. Goldman, and P. C. Canfield, Phys. Rev. B **80**, 174517 (2009).
[18]B. Kalisky, J. R. Kirtley, J. G. Analytis, J.-H. Chu, I. R. Fisher, and K. A. Moler, Phys. Rev. B **83**, 064511 (2011).
[19]C. A. Duran, P. L. Gammel, R. Wolfe, V. J. Fratello, D. J. Bishop, J. P. Rice, and D. M. Ginsberg, Nature (London) **357**, 474 (1992).
[20]See, for example, J. R. Clem and A. Sanchez, Phys. Rev. B **50**, 9355 (1994); E. H. Brandt, *ibid*. **55**, 14513 (1997).
[21]G. Prando, R. Giraud, M. Abdel-Hafiez, S. Aswartham, A. U. B. Wolter, S. Wurmehl, and B. Büchner, arXiv:1207.2457.
[22]M. A. Tanatar, N. Ni, C. Martin, R. T. Gordon, H. Kim, V. G. Kogan, G. D. Samolyuk, S. L. Bud'ko, P. C. Canfield, and R. Prozorov, Phys. Rev. B **79**, 094507 (2009).
[23]H. Q. Yuan, J. Singleton, F. F. Balakirev, S. A. Baily, G. F. Chen, J. L. Luo, and N. L. Wang, Nature (London) **457**, 565 (2009).
[24]R. Prozorov, N. Ni, M. A. Tanatar, V. G. Kogan, R. T. Gordon, C. Martin, E. C. Blomberg, P. Prommapan, J. Q. Yan, S. L. Bud'ko, and P. C. Canfield, Phys. Rev. B **78**, 224506 (2008).
[25]Bing Shen, Peng Cheng, Zhaosheng Wang, Lei Fang, Cong Ren, Lei Shan, and Hai-Hu Wen, Phys. Rev. B **81**, 014503 (2010).
[26]D. S. Inosov *et al*., Phys. Rev. B **81**, 014513 (2010).